Some theoretical results for the convergence of a Glimm-like scheme

Thierry Gallouët, Olivier Hurisse

Some theoretical results for the convergence of a Glimm-like scheme.

T. Gallouët, O. Hurisse

October 16, 2025

Abstract

Front propagation is a challenge in numerical modeling, particularly for multi-fluid or multi-material systems requiring clear material separation. The GRU (Glimm Random Update) scheme, inspired by Glimm's method, has been developed to handle sharp fronts on unstructured 2D/3D meshes. It achieves convergence rates numerically measured between 0.8 and 0.9, which are higher than those of classical first-order schemes, typically limited to 0.5 in the presence of contact discontinuities. Previous work established convergence in probability for planar fronts with uniform velocity but relied on random sequences, whereas practical implementations use low-discrepancy sequences. This study aims to establish new theoretical convergence results for the GRU scheme for 1D non-uniform meshes and uniform front velocity conditions, extending beyond uniform meshes considered previously. More precisely, we prove convergence in probability of order close to one-half when using random sequences on non-uniform meshes, and exact first-order convergence in probability when using low-discrepancy sequences (deterministic) on uniform meshes. Partial results are also obtained for non-uniform meshes, which are of significant practical interest. These findings provide insights into the scheme's behavior with both random and low-discrepancy sequences. Numerical tests are presented to illustrate the theoretical results, with applications to non-uniform meshes, highlighting the scheme's practical relevance.

Contents

1 Introduction

There are numerous numerical strategies for dealing with front propagation in the literature. This is indeed a cornerstone for multi-fluid or multi-material models, for which a clear separation between different materials is mandatory. If the fronts are sharp in the systems of equations of the models, it is known that, from a numerical point of view, approximating sharp fronts is a very tricky problem. Helpful reviews on the subject of sharpening methods and front tracking have recently been proposed in [5, 15]. We restrict ourselves here to methods that are based on Glimm's method, originally proposed in [10], and on front tracking methods as proposed, for instance, in [6] or [1]. An important point to quote is that Glimm's method and its deterministic version [14] are restricted to uniform meshes. These methods have been widely used in the literature for proving the existence of solutions for systems arising from conservation laws. They make the assumption that the approximate solution is piecewise uniform. Then, the key element of these methods is to avoid updating the approximate solution in one cell by using numerical flux balances.

In Glimm's scheme, new values are randomly chosen into the local solutions of each Riemann problem arising at each interface between two neighboring cells. It is thus shown in [10] that such approximate solutions converge towards the exact one with order 1. The schemes derived from the one proposed in [6] do not rely on a random choice. The local Riemann problems are solved until the first wave interaction. Then, wave interaction is solved in order to continue the computation of the approximate solution at later times. The interaction between two shocks and the interaction between a contact wave and a shock can be solved exactly, whereas this is not possible for the interaction between a rarefaction wave and a shock or contact. Hence, rarefaction waves are approximated by a set of uniform values, which introduces non-physical fronts into the rarefaction fan [1, 12].

These two classes of methods are very efficient for computing approximate solutions of systems of conservation laws since they offer a convergence rate of 1 even for linearly degenerate waves. Moreover, fronts are maintained perfectly sharp since no numerical diffusion is introduced. Unfortunately, they are only suitable for 1D problems. Recently, the idea proposed in Glimm's scheme [10] has been taken up and modified in order to handle more complex geometrical settings such as non-uniform 1D meshes and 2D/3D unstructured meshes. This new scheme, nicknamed GRU (Glimm Random Update), was introduced in [13] for dealing with front propagation by using a transport equation of Heaviside functions. It was then extended to the advection of any scalar quantity in [9], and the underlying idea of the scheme can even be applied to the two-phase Euler model (work in progress). As in [10], the GRU scheme is a first-order scheme that relies on a random choice. This strategy allows for perfectly sharp fronts, and effective convergence rates between 0.8 and 0.9 have been measured on both 1D and 2D test cases. It should be recalled that classical first-order schemes based on numerical fluxes offer a convergence rate of $1/2$ as soon as a contact discontinuity occurs in the solution. Figure 1, taken from [13], is reproduced here in order to illustrate the capability of the scheme in simulating the rotation of a non-convex shape in a 2D domain.

In [8], first convergence results were proposed: convergence in probability with order 1 was proved for the propagation of planar fronts in 2D or 3D with uniform velocity. The proof of convergence proposed in [8] relies on the use of a random sequence, while in practice, the random choice in the GRU scheme is performed using low-discrepancy sequences. The latter do not have the same properties as mathematical random sequences. The question, therefore, arises as to how the scheme works with non-random sequences and whether proof of convergence could be obtained for the practical use of the scheme. The question of the use of low-discrepancy sequences was also studied in [14] for Glimm's scheme, and this previous study provided clues to understand the behavior of the GRU scheme.

The aim of the present study is to propose new theoretical convergence results for the GRU scheme when considering 1D meshes and uniform front velocity. Even if these configurations could seem restrictive, the results are very useful for understanding the behavior of the scheme when using either random sequences or low-discrepancy sequences. Moreover, the present study is not restricted to uniform meshes, as in [8]. Therefor, different numerical tools have been used in the proofs. Several classes of non-uniform meshes are considered, which is of prime importance for practical applications. Among the results obtained in this work, it appears that dealing with 1D non-uniform meshes requires careful attention to the choice of random sequences. Pseudo-random sequences are more robust, as they can be applied regardless of mesh quality, even if they yield relatively low accuracy. In contrast, quasi-random sequences—such as low-discrepancy sequences—require caution on certain meshes, where consistency issues may arise. These theoretical results are illustrated by several numerical tests.

The manuscript is organized as follows. The GRU scheme and the previous results are briefly presented in section 2. It should be noted that the GRU scheme is very simple, so this first section is short. Section 3 is devoted to the new theoretical convergence results, while numerical tests are described in section 4.

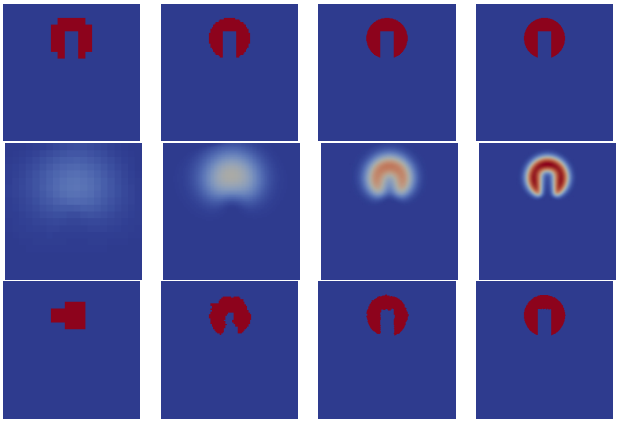

Figure 1: One complete rotation of a non-convex shape on structured meshes. First row: exact initial and final shape, second row: upwind scheme and third row: upwind-GRU scheme. First column: 20×20 cells, second column: 100×100 cells, third column: 400×400 cells and forth column: 1500×1500 cells.

2 Presentation of the GRU projection step

2.1 The GRU projection step.

Let us first present the GRU scheme that as been introduced in [13] and [9] respectively for Heaviside functions and for any scalar function. We assume here a simplified setting with respect to those studied in the previous references [13] and [9]. In the following, attention will be restricted to the 1D case.

We assume here that the quantity $\phi(t,x)$ is advected with velocity V, which is positive ($V > 0$) and which does not depend on space and time:

$$\partial_t(\phi) + V\partial_x(\phi) = 0, \qquad \phi(t=0,x) = \phi_0(x), \tag{1}$$

where $x \mapsto \phi_0(x)$ is the initial condition. For computing approximate solutions of this equation, a fractional step approach based on finite volumes is used. The first step is a convection step, which can be seen as a prediction step. It is assumed that the approximate solutions are computed thanks to the upwind scheme. Let us assume that the approximated values of the solution in all cells i - with a natural increasing numbering of the cells - at iteration n, i.e. at time t^n, are known and denoted by $(\phi_i^n)_i$. The length of cell i is denoted by Δx_i and the time-step at iteration n is Δt^n. Then a first approximated value $\phi_i^{n,*}$ of the solution in cell i at time $t^{n+1} = t^n + \Delta t^n$ is obtained thanks to the mere upwind scheme:

$$\phi_i^{n,*} = (1-\beta_i^n)\phi_i^n + \beta_i^n \phi_{i-1}^n, \qquad \beta_i^n = V\Delta t^n/\Delta x_i. \tag{2}$$

Obviously, the parameter β_i^n has to be smaller than 1 for all cells i in order to ensure the stability of the upwind scheme (2). Thus, for any mesh $(\Delta x_i)_i$ the time step Δt^n at iteration n is chosen in the following according to a CFL (Courant-Friedrichs-Lewy) number $\alpha \in]0,1]$ such that:

$$\Delta t^n = \frac{\alpha}{V}\min_i(\Delta x_i). \tag{3}$$

Then the GRU projection step is applied in each cell on the basis of the predicted value $\phi_i^{n,*}$ defined by (2) and (3). For that purpose, we consider a random number ω^n that follows a uniform distribution in $]0,1[$. Let us define respectively $\phi_{i,m}^n$ and $\phi_{i,M}^n$ as the local minimum and the local maximum of the cell values at time t^n when considering the set composed of: cell i plus the upwind cells with respect to the mass fluxes, see [9] for a more general definition. Since we have here $V > 0$, we get: $\phi_{i,m}^n = \min\left(\phi_{i-1}^n, \phi_i^n\right)$ and $\phi_{i,M}^n = \max\left(\phi_{i-1}^n, \phi_i^n\right)$. The number ω_i^n is introduced as a renormalization of the number ω^n over $(\phi_{i,m}^n, \phi_{i,M}^n)$:

$$\omega_i^n = \phi_{i,m}^n + \omega^n(\phi_{i,M}^n - \phi_{i,m}^n), \tag{4}$$

so that ω_i^n follows the uniform distribution on $(\phi_{i,m}^n, \phi_{i,M}^n)$. The GRU step simply gives for the approximate solution ϕ_i^{n+1} in cell i and at iteration $n+1$:

$$\phi_i^{n+1} = \begin{cases} \phi_{i,m}^n, & \text{if } \phi_i^{n,*} < \omega_i^n, \\ \phi_{i,M}^n, & \text{otherwise;} \end{cases} \tag{5}$$

An important point to be quoted here is that the same ω^n is used for all the cells. This is a cornerstone of such algorithms, as noticed in [2, 3] for the Glimm's scheme. In a practical point of view, ω^n is generally chosen in

low-discrepancy sequences with values in $[0,1]$. They are well-suited for the Glimm's scheme [2, 14, 4] as well as for the GRU step [13, 9], at least on uniform meshes or meshes of industrial interest.

Despite its simplicity, this scheme has very interesting properties for approximating weak solutions of (1) [13, 9]. Discontinuities are maintained perfectly sharp and no intermediate values are created by the scheme. The scheme is not conservative and the approximated discontinuities may not be located at the exact position. Nevertheless, for a simple configuration, it has been proved that the approximate solutions computed with the upwind scheme and the GRU step converge with order 1 in probability [8]. Moreover, in the scalar case with the upwind scheme, the CPU overhead is about 30%, since the upwind scheme has a very low computational cost. For more complex systems (such as the Euler system with a passive scalar, see [13]), the overhead of the GRU step becomes almost negligible compared to the computation of the fluxes.

2.2 Previous convergence results.

First theoretical results for the convergence of the GRU projection step associated with the upwind scheme were presented in [8]. These results were obtained under a very simple setting:

- meshes are Cartesian with the same space-step h in each direction (i.e., 1D meshes are uniform);
- advection velocity is uniform and constant, as in Section 2.1;
- a single planar front is considered by choosing:

$$\phi_0(x) = \begin{cases} 1 & \text{if} \quad x \cdot n > a, \\ 0 & \text{otherwise,} \end{cases}$$

where n is a normal vector and a is a real number. Within this scope, two results were obtained:

(i) The approximate solutions obtained with the upwind-GRU scheme *converge at order* 1 *with probability* 1 to the exact solution.

(ii) The approximate solutions obtained with the upwind-GRU scheme *converge almost surely* to the exact solution.

These results were derived by considering a uniform distribution on $]0,1[$ for the random threshold ω^n, whereas all the numerical experiments presented in previous studies [13, 9] rely on deterministic sequences. From a practical perspective, these random numbers are replaced by two types of sequences: low-discrepancy sequences and pseudo-random sequences (in particular the *rand*() sequences of the C++ library are used here). These sequences are deterministic and only exhibit some of the properties of a mathematically uniform distribution. When using low-discrepancy sequences instead of pseudo-random generators, effective convergence rates between 0.8 and 0.9 have been obtained for a wide range of problems involving discontinuities in 1D and 2D with unstructured meshes. For all these test cases, the GRU step significantly improved the accuracy of the upwind scheme. The use of a pseudo-random generator results in an effective convergence rate of $1/2$, which corresponds to the convergence rate of the upwind scheme alone. Even if no improvement is observed with pseudo-random generators in terms of convergence rate, the fronts are maintained sharp.

3 New theoretical convergence results in 1D

The aim of the present section is to present some extensions of the convergence results of [8] by considering the "deterministic" upwind-GRU scheme (using low-discrepancy sequences for ω^n) and non-uniform meshes. In [8], simple mathematical tools were used considering only random sequences ω^n and uniform meshes. This made it possible to compute the probability density function of the approximated front position. The resulting proof was therefore rather computational in nature but allowed for a more optimal convergence result. Unfortunately, this early proof seems very difficult to extend to non-uniform meshes and to low-discrepancy sequences. To obtain convergence results for these situations, it was necessary, at least as a first step, to rely on other mathematical tools, which sometimes leads to slightly less optimal results.

3.1 Notations and preliminary results

Without loss of generality, and for the sake of simplicity, we assume in this section that $V = 1$. The initial condition is an Heaviside function:

$$\phi_0(x) = \begin{cases} 0 & \text{if} \quad x \geq 0, \\ 1 & \text{otherwise,} \end{cases}$$

defining an initial front located a $x = 0$. At time $t = T_{end}$, the exact solution of system (1) is easily obtained: $\phi(T_{end}, x) = \phi_0(x - T_{end})$. This means that the front is now located at $x = T_{end}$:

$$\phi(T_{end}, x) = \begin{cases} 0 & \text{if} \quad x \geq T_{end}, \\ 1 & \text{otherwise,} \end{cases} \tag{6}$$

The cell i of the mesh corresponds to the segment $]x_{i-1/2}, x_{i+1/2}[$, with $\Delta x_i = x_{i+1/2} - x_{i-1/2}$ its length. Let us also denote by h the largest cell length for the mesh:

$$h = \sup_{j\in\mathbb{Z}}(\Delta x_j), \tag{7}$$

and by r the ratio:

$$r = \inf_{j\in\mathbb{Z}}(\Delta x_j/h). \tag{8}$$

We assume in the following that $r > 0$. The time step defined according to (3) is the same for all time steps. It reads here:

$$\Delta t = \alpha\, r\, h, \tag{9}$$

where $\alpha \in]0,1]$ is the CFL number. With these choices, the number of iterations N_{end} of the scheme needed to reach T_{end} is such that: $T_{end} - \Delta t < \Delta t N_{end} \leq T_{end}$. For the sake of simplicity, let us assume that T_{end} is such that $T_{end} = \Delta t N_{end}$. It should be noted here that this simplification only involves an error in $O(\Delta t)$ or $O(h)$ thanks to the CFL condition. These N_{end} iterations with the GRU scheme described in section 2 are associated with a sequence $(\omega^n)_{1\leq n\leq N_{end}}$ of N_{end} values belonging to $]0,1[$. The approximated initial condition is:

$$\phi_i^0 = \begin{cases} 0 & \text{if} \quad i \geq 0, \\ 1 & \text{otherwise,} \end{cases} \tag{10}$$

and the mesh is adapted to this initial condition by setting $x_{-1/2} = 0$ so that the initial approximated front coincide with the exact front defined by $x \mapsto \phi^0(x)$.

With the settings and assumptions of the present section, the scheme defined in section 2 can be further simplified. For all cell i it then yields:

$$\phi_i^{n,*} = (1-\beta_i)\phi_i^n + \beta_i \phi_{i-1}^n, \quad \beta_i = \Delta t/\Delta x_i \quad \textit{(upwind/prediction step)} \tag{11}$$

$$\phi_i^{n+1} = 0 \quad \text{if} \quad \omega^n > \phi_i^{n,*}, \quad \text{and} \quad \phi_i^{n+1} = 1 \text{ otherwise.} \quad \textit{(GRU/projection step)} \tag{12}$$

Proposition 1. If we assume that at iteration n there exists an index i_n such that $\phi_i^n = 1$ for all $i < i_n$, and $\phi_i^n = 0$ otherwise, then there also exists an index i_{n+1} such that $\phi_i^{n+1} = 1$ for all $i < i_{n+1}$, and $\phi_i^{n+1} = 0$ otherwise. Moreover, we have $i_{n+1} = i_n$ or $i_{n+1} = i_n + 1$.

Proof. Let us assume that there exists a unique cell number i_n such that: $\phi_i^n = 1$ if $i < i_n$, and $\phi_i^n = 0$ otherwise. Due to our previous choices, we simply get from (11) that: $\phi_i^{n,*} = 1$ for all $i < i_n$, $\phi_i^{n,*} = 0$ for all $i > i_n$, and $\phi_{i_n}^{n,*} = \Delta t/\Delta x_{i_n}$ which belongs to $[0,1]$ thanks to (9). Hence we have $\phi_i^{n,*} = \phi_i^n$ for all $i \neq i_n$. As a consequence, following the GRU step (12) - and since ω^n belongs to $]0,1[$ - we obtain easily that $\phi_i^{n+1} = \phi_i^n$ for all $i \neq i_n$. As we also have $\phi_{i_n}^{n+1} \in \{0,1\}$, we get that at iteration $n+1$ the approximate solution is such that there exists $\phi_i^n = 1$ if $i < i_n$, and $\phi_i^n = 0$ otherwise. In fact, the sole cell value that is likely to change from 0 to 1 between iterations n and $n+1$ is that in cell $i = i_n$. We can then conclude that at iteration $n+1$, a unique cell number i_{n+1} can be defined so that: $\phi_i^{n+1} = 1$ if $i < i_{n+1}$, and $\phi_i^{n+1} = 0$ otherwise. This ends the proof of the proposition. •

An additional result can also be obtained from (11)-(12) for the update of the cell number i_n. Indeed, the following relations hold:

$$i_{n+1} = i_n \quad \text{if} \quad \omega^n > \phi_{i_n}^{n,*} = \beta_{i_n}; \qquad i_{n+1} = i_n + 1 \quad \text{otherwise.} \tag{13}$$

Since the initial approximate solution (10) is a projection of an Heaviside function on the mesh, the result of the proposition 1 holds. An approximated front position can be defined from i_n. The location of the approximated front is now denoted by F_n. The cell number i_n clearly gives that $F_n = x_{i_{n-1/2}}$, with $F_0 = 0$ (since $x_{-1/2} = 0$ and thanks to (10)). Relation (13) leads to $F_{n+1} = F_n + X_n \Delta x_{i_n}$, where:

$$X_n = 0 \quad \text{if} \quad \omega^n > \beta_{i_n}\ ; \qquad X_n = 1 \quad \text{otherwise.} \tag{14}$$

With our settings, we have seen that the approximate solutions are projection of Heaviside functions on the mesh. Then, the distance in terms of the L^1-norm between the exact solution and the approximate solution can be reduced to the distance between the exact front location and the approximated front location. The quantity F_n

is thus the quantity that is retained in the following for measuring the error between the exact solution and the approximate solutions.

It should be noted that the results presented in section 3.1 do not depend on the nature of the sequence $(\omega^n)_n$, up to now the only requirement is to have $\omega^n \in]0,1[$ for all n. The consistency and convergence properties of scheme (11)-(12) strongly rely on the properties of the sequences $(\omega^n)_n$. Some results are proposed in the following sections.

3.2 Results for uniform meshes

We investigate here the case of uniform meshes: $\Delta x_i = h$ for all i. This case was already studied in [8] when considering random sequences for $(\omega^n)_n$. This implies great simplifications, in particular we have: $F_{n+1} = F_n + X_n\ h$. In other words, all the sequences that correspond to permutations of 1 to N_{end} values of a given sequence $(\omega^n)_{1\leq n\leq N_{end}}$ will give the same final result for $F_{N_{end}}$. This is the key point for proving results for uniform meshes.

3.2.1 The case of low-discrepancy sequences.

For uniform meshes we easily get that $\beta_i = \alpha$ for each cell i. Let $A_{N_{end}}$ be the set defined by:

$$A_{N_{end}} = card\{n \in \{1,...,N_{end}\};\ 0 < \omega^n < \alpha\}.$$

Thanks to the definition of F_n, we then have: $F_{N_{end}} = A_{N_{end}}\ h$. The distance between the exact front location T_{end} and the final approximated front is thus:

$$|F_{N_{end}} - T_{end}| = |A_{N_{end}} h - N_{end}\Delta t| = h\ N_{end}\ \left|\frac{A_{N_{end}}}{N_{end}} - \alpha\right|. \tag{15}$$

When the sequence $(\omega^n)_n$ is a low-discrepancy sequence, there exists a number $C > 0$ - that only depends on the choice of the sequence - such that for all $\alpha \in]0,1]$:

$$\left|\frac{A_{N_{end}}}{N_{end}} - \alpha\right| \leq C\frac{\ln(N_{end})}{N_{end}}. \tag{16}$$

By introducing inequality (16) in (15), it yields:

$$|F_{N_{end}} - T_{end}| \leq C\ h\ \ln(N_{end}) = C\ h\ \left(\ln(T_{end}) - \ln(\alpha h)\right). \tag{17}$$

From inequality (17), we can conclude that for a low-discrepancy sequence the distance between the approximated front and the exact front tends to zero as $h\ln(h)$.

3.2.2 The case of random sequences.

Let $(\Omega, \mathscr{F}, P)$ be a probability space. Let us consider N_{end} independent and identically distributed real random variables - or IIDRRV in short - $(\zeta_i)_{1\leq i\leq N_{end}}$ following the uniform distribution on $]0,1[$. Formally, building the sequence $(\omega^n)_{1\leq n\leq N_{end}}$ consists in choosing $\omega \in \Omega$ for all n and setting $\omega^n = \zeta_n(\omega)$. It can then be noticed that the variable X_n can be written: $X_n = \varphi(\omega^n) = \varphi(\zeta_n(\omega))$, where φ is the Borelian function defined for $s \in \mathbb{R}$ by:

$$\varphi(s) = 0 \quad \text{is} \quad s > \alpha; \quad \text{and} \quad \varphi(s) = 1 \quad \text{otherwise.}$$

Since $(\zeta_i)_i$ is a set of IIDRRV, $(X_n)_n$ is also a set of IIDRRV. Then the random variable $F_{N_{end}}$ reads:

$$F_{N_{end}} = \sum_{n=1}^{N_{end}} h\ X_n = h\ \sum_{n=1}^{N_{end}} X_n,$$

with the probabilities $P(\{X_n = 0\}) = 1-\alpha$ and $P(\{X_n = 1\}) = \alpha$. The random variable X_n then follows a Bernoulli distribution with parameter α. Therefore, the expectations and the variance of X_n are:

$$E(X_n) = \alpha \quad \text{and} \quad Var(X_n) = E((X_n - E(X_n))^2) = \alpha(1-\alpha). \tag{18}$$

The following inequality is obtained from the proof of the weak law of large numbers (see Equation (6.38) in [7]). Since $(X_n)_n$ is a sequence of IIDRRV, the result of [7] applies, and we obtain for all $\varepsilon > 0$:

$$P\left(\left\{\left|\frac{1}{N_{end}}\sum_{n=1}^{N_{end}} X_n - \alpha\right| \geq \varepsilon\right\}\right) \leq \frac{\alpha(1-\alpha)}{\varepsilon^2\ N_{end}}. \tag{19}$$

Since $N_{end} = T_{end}/(\alpha h)$ we obtain from (19) the following estimation for $F_{N_{end}}$:

$$P\left(\left\{\left|F_{N_{end}} - T_{end}\right| \geq \varepsilon T_{end}/\alpha\right\}\right) \leq h\frac{\alpha^2(1-\alpha)}{\varepsilon^2\, T_{end}}. \tag{20}$$

Let us set $\eta = \varepsilon T_{end}/\alpha$, relation (20) then reads:

$$P\left(\left\{\left|F_{N_{end}} - T_{end}\right| \geq \eta\right\}\right) \leq h\frac{(1-\alpha)T_{end}}{\eta^2}. \tag{21}$$

If we choose $\eta = h^\gamma$ with $\gamma > 0$, (21) gives the estimation:

$$P\left(\left\{\left|F_{N_{end}} - T_{end}\right| \geq h^\gamma\right\}\right) \leq (h)^{1-2\gamma}(1-\alpha)T_{end}, \tag{22}$$

where the right hand side of the inequality tends to zero when h tends to zero if $1-2\gamma > 0 \Leftrightarrow \gamma < 1/2$. This proves that the probability that the distance between the approximated front location and the exact front is greater than h^γ tends to zero if $\gamma < 1/2$. It corresponds essentially to a convergence in probability with an order $1/2$ in term of h.

Remark. In fact, the random variable $F_{N_{end}}$ is the sum of IIDRRV that all follow a Bernoulli distribution with parameter α. Hence, $F_{N_{end}}$ follows a binomial distribution. The first results obtained in [8] rely on this remark. The convergence in probability with order 1 in terms of h has been proven. Nevertheless, these results require calculations that are more complex than the proof proposed here. More details may be found in [8].

3.2.3 Random sequences : an estimation based on Hoeffding's inequality.

The result of section 3.2.2 has been obtained using an inequality arising in from the proof of the weak law of large numbers (see Equation (6.38) in [7]). It is shown in this section that the Hoeffding's inequality [11] can lead to another result. We recall that we have defined $F_{N_{end}} = h\sum_{n=1}^{N_{end}} X_n$ and $T_{end} = N_{end}\Delta t$. For any $\varepsilon > 0$, we first consider here the probability: $P\left(\left\{F_{N_{end}} - T_{end} \geq \varepsilon\right\}\right)$. It should be noted that it corresponds to the probability for the approximated front location to be greater than T_{end} by ε. With respect to the probability considered in section 3.2.2 (see (20) for instance), the absolute value has been removed from the left hand side of the inequality. We set $\tau = \varepsilon/h$, so we have:

$$P\left(\left\{F_{N_{end}} - T_{end} \geq \varepsilon\right\}\right) = P\left(\left\{\sum_{n=1}^{N_{end}} X_n - \frac{T_{end}}{h} \geq \tau\right\}\right).$$

Let us denote $S_{N_{end}} = F_{N_{end}}/h = \sum_{n=1}^{N_{end}} X_n$. Thanks to (18), we have:

$$E(S_{N_{end}}) = E\left(\sum_{n=1}^{N_{end}} X_n\right) = N_{end}\alpha = T_{end}/h,$$

and by choosing $s > 0$ we thus get:

$$P\left(\left\{F_{N_{end}} - T_{end} \geq \varepsilon\right\}\right) = P\left(\left\{S_{N_{end}} - E(S_{N_{end}}) \geq \tau\right\}\right) = P\left(\left\{e^{s(S_{N_{end}} - E(S_{N_{end}}))} \geq e^{(s\tau)}\right\}\right). \tag{23}$$

We recall that the Markov's inequality provides the estimation:

$$P\left(\left\{e^{s(S_{N_{end}} - E(S_{N_{end}}))} \geq e^{(s\tau)}\right\}\right) \leq e^{-(s\tau)}\, E\left(e^{s(S_{N_{end}} - E(S_{N_{end}}))}\right),$$

which, together with relation (23) and by using the fact that the X_n are independent, gives:

$$P\left(\left\{F_{N_{end}} - T_{end} \geq \varepsilon\right\}\right) \leq e^{-(s\tau)}\, E\left(e^{s(S_{N_{end}} - E(S_{N_{end}}))}\right) = e^{-(s\tau)} \prod_{n=1}^{N_{end}} E\left(e^{s(X_n - E(X_n))}\right). \tag{24}$$

Since the random variable X_n follows a Bernoulli distribution with parameter α, see (14), we have:

$$E\left(e^{s(X_n - E(X_n))}\right) = E\left(e^{s(X_n - \alpha)}\right) = (1-\alpha)e^{-s\alpha} + \alpha e^{s(1-\alpha)} = e^{-s\alpha}\left(1 - \alpha + \alpha e^s\right),$$

and thanks to the lemma proposed in appendix 6.1 we obtain the following inequality:

$$E\left(e^{s(X_n - E(X_n))}\right) = e^{-s\alpha}\left(1 - \alpha + \alpha e^s\right) \leq e^{s^2/8}. \tag{25}$$

Introducing inequality (25) in (24) leads to:

$$P\left(\left\{F_{N_{end}} - T_{end} \geq \varepsilon\right\}\right) \leq e^{-(s\tau)}\, \left(e^{s^2/8}\right)^{N_{end}} = e^{\left(N_{end}s^2/8 - s\tau\right)}. \tag{26}$$

The polynomial $s \mapsto N_{end}s^2/8 - s\tau$, for $s \geq 0$, reaches its minimum for $s = 4\tau/N_{end} \geq 0$, and its value is $-2\tau^2/N_{end}$. Since inequality (26) holds for any $s \geq 0$, it holds for $s = 4\tau/N_{end}$. Therefore we have:

$$P\left(\left\{F_{N_{end}} - T_{end} \geq \varepsilon\right\}\right) \leq e^{\left(-\frac{2\tau^2}{N_{end}}\right)} = e^{\left(-\frac{2\alpha\varepsilon^2}{hT_{end}}\right)}. \tag{27}$$

In the same way, one can get the inequality:

$$P\left(\left\{T_{end} - F_{N_{end}} \geq \varepsilon\right\}\right) \leq e^{\left(-\frac{2\alpha\varepsilon^2}{hT_{end}}\right)}, \tag{28}$$

and, thus, by using both (27) and (28) the following inequality is obtained:

$$P\left(\left\{|F_{N_{end}} - T_{end}| \geq \varepsilon\right\}\right) \leq 2\, e^{\left(-\frac{2\alpha\varepsilon^2}{hT_{end}}\right)}, \tag{29}$$

By setting $\varepsilon = h^\gamma$ with $\gamma > 0$, relation (29) gives the counterpart of inequality (22):

$$P\left(\left\{|F_{N_{end}} - T_{end}| \geq h^\gamma\right\}\right) \leq 2\, e^{\left(-\frac{2\alpha h^{2\gamma-1}}{T_{end}}\right)}, \tag{30}$$

As for the estimation of section 3.2.2, the convergence in probability of the approximated front to the exact front is achieved for $\gamma < 1/2$.

3.3 Results for non-uniform meshes

Non-uniform meshes are considered now. Hence, on the contrary to section 3.2, the sequences that correspond to permutations of 1 to N_{end} values of a given sequence $(\omega^n)_{1\leq n\leq N_{end}}$ may not give the same final result for $F_{N_{end}}$. This also means that what happens at iteration n depends on what happened at all iterations $i < n$.

In [8], simple mathematical tools were used considering only random sequences ω^n and uniform meshes. This made it possible to compute the probability density function of the approximated front position. The resulting convergence proof was therefore rather computational in nature but allowed for a more optimal convergence result. Unfortunately, this early proof seems not easy to extend to non-uniform meshes and to low-discrepancy sequences. To propose convergence results for these situations, we choose here, at least as a first step, to rely on other mathematical tools, which sometimes leads to slightly less optimal results.

3.3.1 The case of low-discrepancy sequences.

No result has been found so far when considering any type of non-uniform mesh. We propose to focus in this section on some specific classes of meshes. A main difficulty lies in the fact that a subsequence of a low-discrepancy sequence is not, *a priori*, a low-discrepancy sequence, in contrast to random sequences, for which any subsequence remains random (provided the extraction is independent).

Proof of convergence for "odd-even" meshes.
Let us define the meshes such that: $\Delta x_i = h$ if i is odd, and $\Delta x_i = h/a$ if i is even, where $a > 1$. For these "odd-even" meshes, numerical experiments exhibit a loss of consistency when using the scheme as described in section (2). This point is developed in section 4 in a numerical point of view. For recovering the consistency of the GRU scheme on these "odd-even" meshes, it has to be slightly modified. We now consider two different low-discrepancy sequences: a sequence $(\widetilde{\omega}^n)_{n\geq 0}$ for odd cells and a sequence $(\overline{\omega}^n)_{n\geq 0}$ for even cells. The GRU step of section 2 is then modified.

Let us consider an approximate solution at iteration n such that: $\phi_i^n = 1$ for all $i < I^n$, and $\phi_i^n = 0$ otherwise. When the front faces an odd cell, i.e. when I^n is odd, the local threshold ω_i^n (see (4)) is computed thanks to:

$$\omega_i^n = \phi_{i,m}^n + \widetilde{\omega}^{p(n)}(\phi_{i,M}^n - \phi_{i,m}^n),$$

where $p(n)$ counts the number of time I^n has been odd during the first $n-1$ iterations. When the front faces an even cell, i.e. when I^n is even, the local threshold ω_i^n reads:

$$\omega_i^n = \phi_{i,m}^n + \overline{\omega}^{q(n)}(\phi_{i,M}^n - \phi_{i,m}^n),$$

where $q(n)$ counts the number of time I^n has been even during the first $n-1$ iterations. Obviously, we have $p(n) + q(n) = n$. Moreover, if I^n is odd (resp. even) we have $p(n+1) = p(n) + 1$ and $q(n+1) = q(n)$ (resp. $p(n+1) = p(n)$ and $q(n+1) = q(n) + 1$). The most important point here is to notice that $p(n)$ and $q(n)$ have been introduced to desynchronize the two sequences so that all their elements are used. We can now use the same type of proof than in section 3.2.1.

For "odd-even" meshes, we have $\beta_i = \alpha$ if i is odd and $\beta_i = \alpha/a$ if i is even. For any sequence $(\widetilde{\omega}^n)_{1\leq n\leq p(N_{end})}$, $\widetilde{A}_{p(N_{end})}$ is the number of values $\widetilde{\omega}^n$ less than α/a:

$$\widetilde{A}_{p(N_{end})} = card\{j \in \{1,...,p(N_{end})\};\ 0 < \widetilde{\omega}^j < \alpha/a\}.$$

In a similar way, for any sequence $(\overline{\omega}^n)_{1\leq n\leq q(N_{end})}$, $\overline{A}_{p(N_{end})}$ is the number of values $\overline{\omega}^n$ less than α:

$$\overline{A}_{q(N_{end})} = card\{j \in \{1,...,q(N_{end})\};\ 0 < \overline{\omega}^j < \alpha\}.$$

Now, thanks to the definition of F_n, we have: $F_{N_{end}} = \widetilde{A}_{p(N_{end})}\ h\ +\ \overline{A}_{q(N_{end})}\ h/a$. We recall here that we have $p(N_{end}) + q(N_{end}) = N_{end}$. Therefore, the distance between the exact front location T_{end} and the final approximated front is thus:

$$|F_{N_{end}} - T_{end}| = \left|\left(\widetilde{A}_{p(N_{end})}\ h - p(N_{end})\Delta t\right)\ +\ \left(\overline{A}_{q(N_{end})}\ \frac{h}{a} - q(N_{end})\Delta t\right)\right|, \tag{31}$$

where $\Delta t = \alpha h/a$ according to (9) (i.e. the time step is chosen with respect to the smallest - even - cells). Hence, we get the inequalities:

$$|F_{N_{end}} - T_{end}| \leq \left|\widetilde{A}_{p(N_{end})}\ h - p(N_{end})\Delta t\right|\ +\ \left|\overline{A}_{q(N_{end})}\ \frac{h}{a} - q(N_{end})\Delta t\right|, \tag{32}$$

$$|F_{N_{end}} - T_{end}| \leq hp(N_{end})\left|\frac{\widetilde{A}_{p(N_{end})}}{p(N_{end})} - \frac{\alpha}{a}\right| + hq(N_{end})\left|\frac{\overline{A}_{q(N_{end})}}{q(N_{end})} - \alpha\right|, \tag{33}$$

which thanks to bound (16) gives:

$$|F_{N_{end}} - T_{end}| \leq C'h(\ln(p(N_{end})) + \ln(q(N_{end}))) \leq 2C'h\ln(N_{end}) \tag{34}$$

where C' is a non-negative number which only depends on the choice of the low-discrepancy sequence. Since $N_{end} \leq aT_{end}/(\alpha h)$, we finally obtain the bound:

$$|F_{N_{end}} - T_{end}| \leq 2C'h(\ln(aT_{end}) - \ln(\alpha h)). \tag{35}$$

We can conclude from (35) that using the specific algorithm involving two low-discrepancy sequences, the distance between the approximated front and the exact front tends to zero at least as $h\ln(h)$ on "odd-even" meshes.

Remark. When using only one low-discrepancy sequence on "odd-even" meshes, inequality (16) does not hold because the regular scheme of section 2 uses two subsequences which are no more low-discrepancy sequences. This point will be illustrated by numerical experiments in section 4.

Remark. One could use the same sequence for both cell types, i.e. $(\widetilde{\omega})^n = (\overline{\omega})^n$, the main point in this section is to desynchronize how values are selected for small and large cells by using separate counters $p(n)$ and $q(n)$.

Extension of the proof to more general "two-size meshes".
It is important to note that in the previous proof the number of even cells, the number of odd cells and their alternation are absolutely irrelevant. The most important point is to desynchronize the use of the sequences on the small and big cells. As a consequence, the proof can easily be extended to a more general class of meshes which is the following:

- Let $\mathbb{Z}_1$ and $\mathbb{Z}_2$ be two subsets of $\mathbb{Z}$ such that $\mathbb{Z} = \mathbb{Z}_1 \cup \mathbb{Z}_2$ and $\mathbb{Z}_1 \cap \mathbb{Z}_2 = \emptyset$.
- Cells $i \in \mathbb{Z}_1$ have a size $\Delta x_i = h/a$ with $a > 1$, and cells $i \in \mathbb{Z}_2$ have a size $\Delta x_i = h$.

Extension of the proof to more general block-shaped meshes.

Let us now consider meshes built using blocks of cells of the same size. It is recalled that due to the assumptions of section 3.1, the front can not travel back: if i_n is its position at iteration n (i.e. $\phi_j^n = 1$ for all $j < i_n$) then at iteration $n+1$ we get $i_{n+1} \in \{i_n, i_n + 1\}$.

For N cells, we define a set of M contiguous intervals $R_p = [\![B_p, E_p]\!]$ with: $B_p < E_p$, $B_{p+1} = E_p + 1$, $B_1 = 0$ and $E_M = N$; so that we have $\cup_{p=1}^{M} R_p = [\![1, N]\!]$. We assume now that:

- for all cells i in R_p, the mesh size is the same: $\Delta x_i = h_p$;
- for all p in $[\![1, M]\!]$, $h \geq h_p \geq h/a$ with $a > 1$;
- the initial front is located before cell B_1 which means that $i^0 = 0$.

The time step is then chosen in agreement with cells of size h/a: $\Delta t = \alpha h/a$. Thus for $i \in R_p$ the parameter $\beta_i = \Delta t/\Delta x_i$:

$$\beta_i = \frac{\alpha h}{a h_p} = \frac{\Delta t}{h_p} = \beta^p.$$

Let us define N_p the number of iterations needed by the scheme to cross the block associated with R_p, i.e. if $i_k = B_p$ at a given iteration k then $i_{k+N_p} = B_{p+1} = E_p + 1$. Among these N_p iterations from k to $k+N_p$, $A^k_{N_p}$ iterations correspond to a jump forward of size h_p of the front with:

$$A^k_{N_p} = card\{n \in \{k, ..., k+N_p\};\ 0 < \omega^n < \alpha h/(a h_p)\}.$$

We assume that the domain is large enough for the approximated front to remain in the domain until N_{end} iterations, for instance by ensuring that M fullfils:

$$\sum_{p=1}^{M} h_p(E_p + 1 - B_p) > N_{end} h,$$

where $E_p + 1 - B_p$ represents the number of cells in R_p. For the sake of simplicity, the final time T_{end} is assumed to be such that there exists a $M_{end} \in [\![1, M]\!]$ fulfilling $T_{end} = \Delta t \sum_{p=1}^{M_{end}} N_p$, which means that all the blocks $p \in [\![1, M_{end}]\!]$ have been entirely crossed.

After N_{end} iterations, the approximated front is located at $F_{N_{end}} = \sum_{p=1}^{M_{end}} h_p A^{k_p}_{N_p}$, where k_p is the first iteration for which $i^{k_p} = B_p$ (i.e. the iteration at which the approximated front enters the block R_p). Since the exact front is located at:

$$T_{end} = \sum_{p=1}^{M_{end}} N_p \Delta t = \sum_{p=1}^{M_{end}} N_p \beta^p h_p$$

we have:

$$T_{end} - F_{N_{end}} = \sum_{p=1}^{M_{end}} h_p \left(N_p \beta^p - A^{k_p}_{N_p} \right).$$

Therefore, we obtain the inequalities:

$$\left| T_{end} - F_{N_{end}} \right| \leq \sum_{p=1}^{M_{end}} h_p \left| N_p \beta^p - A^{k_p}_{N_p} \right| \leq h \sum_{p=1}^{M_{end}} N_p \left| \beta^p - \frac{A^{k_p}_{N_p}}{N_p} \right|,$$

which by using bound (16) leads to:

$$\left| T_{end} - F_{N_{end}} \right| \leq h \sum_{p=1}^{M_{end}} C_{N_p} \ln(N_p).$$

where C_{N_p} is the constant arising in bound (16). If we assume that there exists a constant C such that $C_{N_p} < C$ for all p, we finally have:

$$\left| T_{end} - F_{N_{end}} \right| \leq h\, C\, M_{end}\ \ln(N_{end}). \tag{36}$$

Let us make an assumption on the size of the blocks P_p: there exist b such that for all p we have

$$E_p + 1 - B_p \geq b N^{\gamma}_{end}, \tag{37}$$

with $0 < \gamma \leq 1$. Thanks to the definition of the intervals R_p, we get that:

$$\sum_{p=1}^{M_{end}} (E_p + 1 - B_p) = \sum_{p=1}^{M_{end}} (B_{p+1} - B_p) = B_{M_{end}+1} - B_1 = E_{M_{end}},$$

and thus that by summing relations (37) over p we have:

$$E_{M_{end}} \geq b N^{\gamma}_{end} M_{end}.$$

Now, considering the setting of our problem, there exists a number b' depending on a and α such that:

$$E_{M_{end}} \leq b' N_{end}.$$

Therefore we obtain the following bound for the number of blocks M_{end}:

$$M_{end} \leq \frac{b'}{b} N^{1-\gamma}_{end}. \tag{38}$$

For the class of meshes defined by (37), the number of blocks M_{end} increases slower than the size of the mesh N_{end}. Introducing bound (38) into inequality (36) then yields:

$$\left|T_{end} - F_{N_{end}}\right| \leq h\, C\, \frac{b'}{b}\, N_{end}^{1-\gamma}\, \ln(N_{end}).$$

Since $N_{end} \leq aT_{end}/(\alpha h)$, the previous inequality can also be written in terms of the mesh size h:

$$\left|T_{end} - F_{N_{end}}\right| \leq C' \left(\frac{aT_{end}}{\alpha}\right)^{1-\gamma} h^{\gamma} \left(\ln\left(\frac{aT_{end}}{\alpha}\right) - \ln(h)\right). \tag{39}$$

We can conclude from (39) that using the specific algorithm involving two low-discrepancy sequences, the distance between the approximated front and the exact front tends to zero at least as $h\ln(h)$ on block-shaped meshes.

Some important remarks must be added. Firstly, when M_{end} is independent of N_{end}, inequality (36) gives a convergence in probability in $h\ln(h)$. This is an interesting setting since it corresponds to the classical process for mesh building in real simulations. Indeed, for real applications refinement is classically performed while keeping fixed the space dimension of the blocks or equivalently the number of blocks in the mesh. In the general setting described above, the size of the blocks can be refined together with N_{end}. Secondly, when γ equals zero the "odd-even" case is recovered here and inequality (39) no more guaranties the convergence in probability of the approximated front to the exact one. Several numerical experiments are presented in section 4 for illustrating these results.

3.3.2 The case of random sequences.

We use here the same probabilistic framework that the one introduced in section 3.2. But on the contrary to the latter, the variable X_n can be written: $X_n = \varphi_{i_n}(\omega^n) = \varphi_{i_n}(\zeta_n(\omega))$, where φ_{i_n} is the Borelian function defined for $s \in \mathbb{R}$ by:

$$\varphi_{i_n}(s) = 0 \quad \text{is} \quad s > \beta_{i_n}; \quad \text{and} \quad \varphi_{i_n}(s) = 1 \quad \text{otherwise.}$$

For the position of the approximated front at T_{end}, we introduce the random variable $Y_n = \Delta x_{i_n} X_n$ which corresponds to the displacement of the approximated front at iteration n. So that we have:

$$F_{N_{end}} = \sum_{n=1}^{N_{end}} \Delta x_{i_n}\, X_n = \sum_{n=1}^{N_{end}} Y_n.$$

The variable Y_n depends on ω^n. But, on the contrary to section 3.2, it also depends on i_n which depends on the sub-sequence $(\omega^i)_{i<n}$. Therefore, the set $(Y_n)_n$ is not a set of IIDRRV. This adds some difficulties to get theoretical results.

Let us first compute the expectation of Y_n:

$$E(Y^n) = E(\Delta x_{i_n} \varphi_{i_n}(\omega^n)) = E\left(\sum_{j=1}^{N_{end}} 1_{\{(i_n=j)\,\cap\,(i_n\leq n)\}}\, \Delta x_j \varphi_j(\omega^n)\right) = \sum_{j=1}^{N_{end}} E\left(1_{\{(i_n=j)\,\cap\,(i_n\leq n)\}}\, \Delta x_j \varphi_j(\omega^n)\right).$$

At iteration n, the approximated front is located between abscissa $x_{-1/2}$ and $x_{n-1/2}$. Therefore, in the two last expressions of the equation above, the sum on j has been written from 1 to $N_{end} \geq n$, but it has been expressed that i_n must be less or equal than n in the indicator function $1_{\{i_n=j\,\cap\, i_n\leq n\}}$. Since ζ_n does not depend on $(\zeta_1, ..., \zeta_{n-1})$, the random variables $1_{\{(i_n=j)\,\cap\,(i_n\leq n)\}}$ and $\varphi_j(\omega^n)$ are independent for all j and the expectation $E(Y^n)$ can be written:

$$E(Y^n) = \sum_{j=1}^{N_{end}} E\left(1_{\{(i_n=j)\,\cap\,(i_n\leq n)\}}\, E\left(\Delta x_j \varphi_j(\omega^n)\right)\right).$$

Moreover, we have:

$$E\left(\Delta x_j \varphi_j(\omega^n)\right) = \beta_i \Delta x_i = \Delta t, \quad \text{and} \quad P\left(1_{\{(i_n=j)\,\cap\,(i_n\leq n)\}}\right) = 1, \tag{40}$$

so that we finally get:

$$\forall n, \quad E(Y^n) = \Delta t. \tag{41}$$

It should be noted that for a constant and uniform velocity V, the expectation (41) would become $V\Delta t$ (in (41) we have $V = 1$). This means that for each time step, the expected displacement of the approximate front is equal to the displacement of the exact front during the corresponding time Δt. In other words, there is no bias in the velocity of of displacement the approximated front.

The variance of Y^n is defined as $Var(Y^n) = E((Y^n - E(Y^n))^2)$, or using former result (41): $Var(Y^n) = E((Y^n - \Delta t)^2)$. Then, using the same arguments than for the expectation $E(Y^n)$, we get:

$$Var(Y^n) = \sum_{j=1}^{N_{end}} E\left(1_{\{(i_n=j) \cap (i_n \leq n)\}} \ (\Delta x_j \varphi_j(\omega^n) - \Delta t)^2\right) = \sum_{j=1}^{N_{end}} P\left(1_{\{(i_n=j) \cap (i_n \leq n)\}}\right) E\left((\Delta x_j \varphi_j(\omega^n) - \Delta t)^2\right). \tag{42}$$

Let us now detail the last expectation in the sum of the right hand side term in the relation above. With probability $1-\beta_i$, we have $\omega^n > \beta_j$ and thus $(\Delta x_j \varphi_j(\omega^n) - \Delta t)^2 = (\Delta t)^2$. Conversely, with probability β_j we have $\omega^n \leq \beta_j$, which leads to $(\Delta x_j \varphi_j(\omega^n) - \Delta t)^2 = (\Delta x_j - \Delta t)^2$. Therefore, we obtain:

$$E\left((\Delta x_j \varphi_j(\omega^n) - \Delta t)^2\right) = (\Delta t)^2(1-\beta_j) + (\Delta x_j - \Delta t)^2 \beta_j,$$

and since $\beta_j = \Delta t / \Delta x_j$:

$$E\left((\Delta x_j \varphi_j(\omega^n) - \Delta t)^2\right) = \Delta t^2 \frac{1-\beta_j}{\beta_j} \leq \Delta t^2 \frac{1-\beta_j}{\beta_j} \tag{43}$$

where r has been defined by (8). Thanks to the definition of r and to definition (9) for the time-step, we have:

$$\frac{1}{\beta_j} = \frac{\Delta x_j}{\Delta t} \leq \frac{h}{\Delta t} = \frac{1}{\alpha\, r},$$

Equation (43) then gives the inequality:

$$E\left((\Delta x_j \varphi_j(\omega^n) - \Delta t)^2\right) \leq \Delta t^2 \frac{1-\alpha\, r}{\alpha\, r},$$

and variance (42) fulfills the inequality:

$$\forall n, \quad Var(Y^n) \leq \Delta t^2 \frac{1-\alpha\, r}{\alpha\, r}. \tag{44}$$

Let us now turn to the computation of the co-variance term: $covar(Y^n, Y^m) = E((Y^n - E(Y^n))(Y^m - E(Y^m)))$ with $m < n$. Using the definition of $covar(Y^n, Y^m)$, we have:

$$covar(Y^n, Y^m) = E\left(\left(\sum_{j=1}^{N_{end}} 1_{\{(i_n=j) \cap (i_n \leq n)\}} \ (\Delta x_j \varphi_j(\omega^n) - \Delta t)\right)\left(\sum_{k=1}^{N_{end}} 1_{\{(i_m=k) \cap (i_m \leq m)\}} \ (\Delta x_k \varphi_k(\omega^m) - \Delta t)\right)\right),$$

and thus:

$$covar(Y^n, Y^m) = \sum_{j=1}^{N_{end}} \sum_{k=1}^{N_{end}} E\left(1_{\{(i_n=j) \cap (i_n \leq n)\}} \ 1_{\{(i_m=k) \cap (i_m \leq m)\}} \ (\Delta x_k \varphi_k(\omega^m) - \Delta t) \ (\Delta x_j \varphi_j(\omega^n) - \Delta t)\right).$$

Here again, we use the fact that ζ_n does not depend on $(\zeta_1, ..., \zeta_{n-1})$. In particular for $m < n$, ζ_n does not depend on $(\zeta_1, ..., \zeta_m)$. Therefore the random variables:

$$1_{\{(i_n=j) \cap (i_n \leq n)\}} \ 1_{\{(i_m=k) \cap (i_m \leq m)\}} \ (\Delta x_k \varphi_k(\omega^m) - \Delta t) \quad \text{and} \quad (\Delta x_j \varphi_j(\omega^n) - \Delta t)$$

are independent for $m < n$. We thus have:

$$covar(Y^n, Y^m) = \sum_{j=1}^{N_{end}} \sum_{k=1}^{N_{end}} E\left(1_{\{(i_n=j) \cap (i_n \leq n)\}} \ 1_{\{(i_m=k) \cap (i_m \leq m)\}} \ (\Delta x_k \varphi_k(\omega^m) - \Delta t)\right) \ E\left((\Delta x_j \varphi_j(\omega^n) - \Delta t)\right).$$

However, thanks to former result (40) we know that: $E\left((\Delta x_j \varphi_j(\omega^n) - \Delta t)\right) = 0$ for all j so that we finally get:

$$\forall n, \ \forall m < n, \quad covar(Y^n, Y^m) = 0. \tag{45}$$

Inequality for the variance (44) and the computation of the covariance (45) are now used for obtaining an estimation for the distance between the approximated front position $F_{N_{end}}$ and the exact front position T_{end}. Let us first compute $E\left((F_{N_{end}} - T_{end})^2\right)$:

$$E\left((F_{N_{end}} - T_{end})^2\right) = E\left(\left(\sum_{n=1}^{N_{end}} (Y_n - \Delta t)\right)^2\right) = E\left(\left(\sum_{n=1}^{N_{end}} (Y_n - E(Y_n))\right)^2\right),$$

where the relation $T_{end} = N_{end}\Delta t$ introduced in section 3.1 and result (41) have been used. By using result (45) for the covariance, we get:

$$E\left((F_{N_{end}} - T_{end})^2\right) = \sum_{n=1}^{N_{end}} var(Y_n) + \underbrace{\sum_{n=1,m=1,m\neq n}^{n=N_{end},m=N_{end}} covar(Y^n, Y^m)}_{=0 \text{ eq. (45)}} = \sum_{n=1}^{N_{end}} var(Y_n).$$

Then, using inequality (44) yields:

$$E\left((F_{N_{end}} - T_{end})^2\right) \leq N_{end}\Delta t^2 \frac{1-\alpha\, r}{\alpha\, r} = T_{end}\Delta t \frac{1-\alpha\, r}{\alpha\, r} = T_{end}\alpha r h \frac{1-\alpha\, r}{\alpha\, r}$$

The Bienayme-Tchebychev inequality can then be applied and we get for all $\eta > 0$:

$$P\left(\left\{\left|F_{N_{end}} - T_{end}\right| \geq \eta\right\}\right) \leq \frac{1}{\eta^2} E\left((F_{N_{end}} - T_{end})^2\right) \leq \frac{h}{\eta^2}\, T_{end}\alpha r \frac{1-\alpha\, r}{\alpha\, r}. \tag{46}$$

For $\eta = h^\gamma$, inequality (46) leads to:

$$P\left(\left\{\left|F_{N_{end}} - T_{end}\right| \geq h^\gamma\right\}\right) \leq h^{1-2\gamma}\, T_{end}\alpha r \frac{1-\alpha\, r}{\alpha\, r}.$$

This proves that the probability that the distance between the approximated front location and the exact front location is greater than h^γ tends to zero if $\gamma < 1/2$. It corresponds essentially to a convergence in probability with an order $1/2$ in term of h.

4 Numerical experiments

Several theoretical results were presented in section 3. They concern the GRU scheme introduced in [13, 9] for which a first convergence result was proposed in [8]. The purpose of this section is to provide a numerical illustration of the theoretical results from the previous sections. Several convergence studies are then carried out here for a simple 1D case of front propagation. As the scheme is not widely known, it seems important to start this section with a more general example (section 4.1). This first example will provide the reader with an overview of the capabilities of the GRU scheme which is not restricted to the simple setting studied in the previous sections. The following sections are dedicated to illustrating the properties introduced in the section 3 for front propagation. Section 4.2 deals with uniform meshes, while section 4.3 deals with non-uniform meshes.

For the test cases of sections 4.2 and 4.3, the random numbers are obtained thanks to the *rand()* function of the *stdlib* librairy of the langage *C/C++*. The latter is a pseudo-random generator. The low discrepancy sequences are built using the Linear Congruential Generator (LCG) with specific (but classical) parameters:

$$\omega^{n+1} = mod(\omega^n + c, 1), \quad \text{with} \quad c = \frac{\sqrt{5}-1}{2} \quad \text{and} \quad \omega^0 \in]0,1[.$$

We choose here the seed value $\omega^0 = 0.05$. The LCG sequences are used as quasi-random generators. The settings for the initial value problem are those depicted in the beginning of section 3. The velocity is equal to 1. The initial solution consists in a front located at $x = 0.3$ (i.e. $\phi(t=0,x) = 1$ for all $x < 0.3$ and $\phi(t=0,x) = 0$ otherwise). We consider the final time $0.5\ s$ so that the final front is located at $x = 0.3 + 0.5 = 0.8$. The CFL is set to $\alpha = 0.5$.

4.1 A first demonstration test case

This test case was first published in [9] by the authors. It is reproduced here in order to give an example of a simulation with the GRU scheme. It corresponds to computing approximate solutions of system:

$$\begin{cases} \partial_t(\rho) + \partial_x(\rho U) = 0, \\ \partial_t(\rho\phi) + \partial_x(\rho U \phi) = 0, \end{cases} \tag{47}$$

with an initial condition for the scalar quantity $\phi(t,x)$. System (47) involves a non-negative density $\rho(t,x) > 0$ and a velocity $U(t,x)$ which are assumed to be bounded. Both are given in an analytical manner and the sole remaining unknown is $\phi(t,x)$. A class of solutions for system (47) was proposed in [9]. We choose here one of these solutions for which the velocity is positive, constant and decreasing along x: $U(x) > 0$ and $dU/dx < 0$. The initial solution for ϕ, i.e. $\phi(t=0,x)$, is piecewise regular and it is shown in figure 2 (dotted black line). It should be remarked that this initial solution presents two discontinuities. The final solution is also plotted in figure 2 (dashed black line) and it corresponds to a compression and translation of $\phi(t=0,x)$.

Approximate solutions computed with the GRU scheme associated with an upwind-type scheme are plotted in figure 2 for several uniform meshes. The number ω^n are obtained here using a low-discrepancy sequence generated using the Linear Congruential Generator. For this test case, a convergence study showed that the approximate solutions converge towards the exact solution with an effective order of 0.82 while the upwind scheme only gives a effective convergence rate of $1/2$ due to the presence of discontinuities in the profile of the solution. The GRU scheme thus largely improves the accuracy of the approximate solution. In particular, fronts are maintained perfectly sharp when using the GRU scheme. More details may be found in [9], which also includes 2D test cases on unstructured meshes.

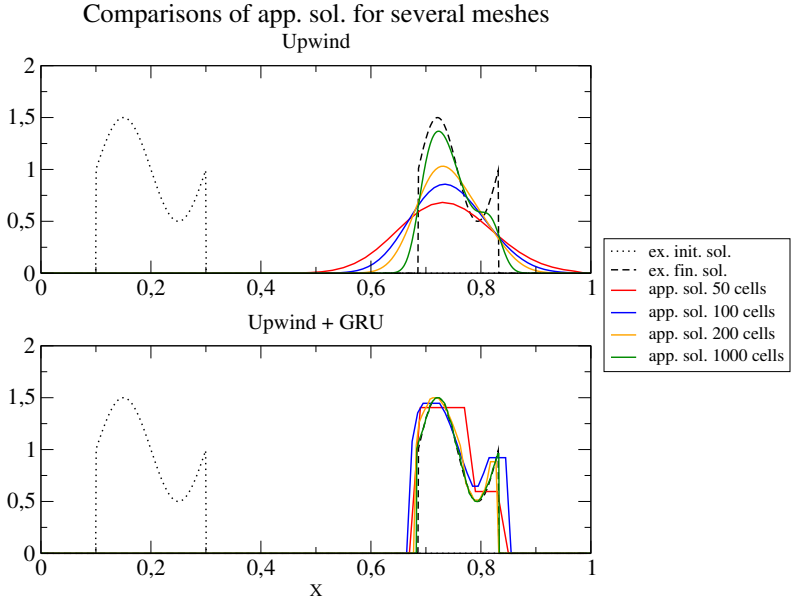

Figure 2: approximate solutions obtained with the sole upwind scheme (top) and with the upwind scheme coupled to the GRU projection step. The initial solution and the final solution are plotted respectively with a dotted black line and a dashed black line.

4.2 Front propagation on uniform meshes

Let us first compare the approximate solutions computed with the sole upwind scheme (without GRU step) and with the upwind scheme coupled to the GRU step while using rand() or LCG sequences. The approximate solutions are plotted in figure 3 for meshes with 200 and 400 cells. Fronts are maintained perfectly sharp with the GRU scheme, while the upwind scheme smears the front over several cells. Convergence curves are plotted on figure 4 for the set of meshes with 25×2^k, $k \in [\![0, 11]\!]$ cells. It can clearly be seen that the use of rand() sequences does not improve much the effective convergence rate even if the front remains sharp. On the contrary, the use of LCG sequences leads to almost perfect accuracy. For all the tests we performed here, the error in the front position is either 0 or 1 cell (of size h). For the former case, the error is not plotted (because it is not defined on a logarithmic scale), which explains that some points (i.e., meshes) are missing for the blue curve in figure 4. For the latter case, the associated points of the blue curve belong to the line $\log(\text{err}) = \log(h)$.

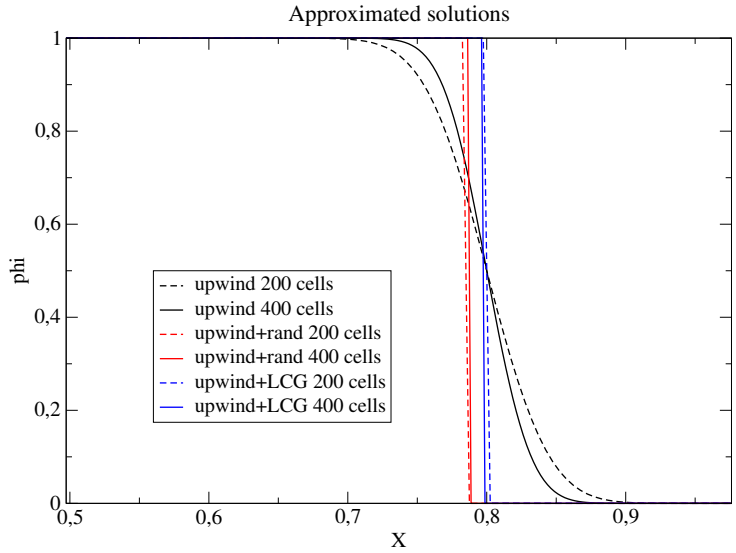

Figure 3: approximate solutions obtained with the upwind scheme and with the upwind scheme associated with the GRU step using rand() or LCG sequences.

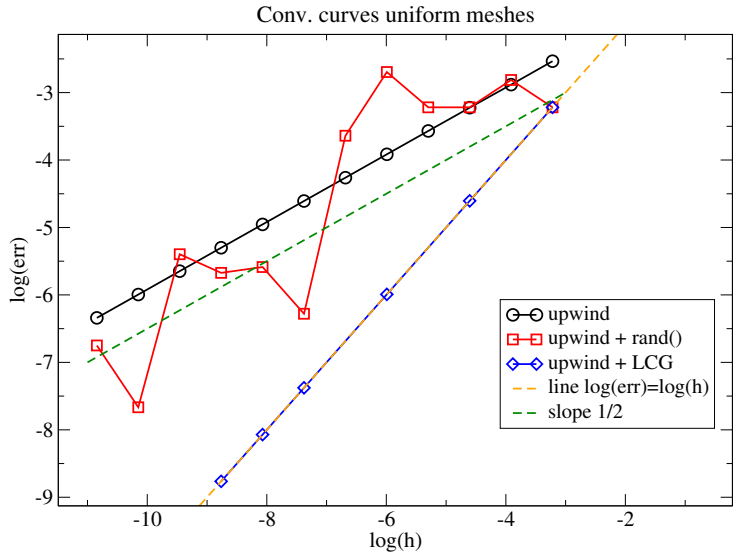

Figure 4: Convergence curves for the upwind scheme and with the upwind scheme associated with the GRU step using rand() or LCG sequences.

The results with the rand() sequences described above exhibit poor quality, while the corresponding theoretical results of section 3 show a better convergence rate. In fact, we use here a single sequence for each mesh, while theoretical results are statistical. Recovering the theoretical (statistical) results would require unaffordable computational effort. Indeed, for a given mesh with N_c cells, we should perform K_t tries with different random values for each iteration, then each of these results should be pursued in the next iteration by another K_t tries, and so on. Since the number of iterations increases with N_c, this procedure would require $\sim (K_t)^{N_c}$ simulations for a given mesh.

We thus perform a weak form of this statistical numerical experiment. For every single mesh, the approximate solution is computed using several different rand() sequences. Each sequence gives only one front position. Then, the average position of the approximated front and its standard deviation are computed. We use N_c different tries of the rand() sequence for each mesh with N_c cells. This appears to be enough, at least for small meshes, in our case for $N_c < 6400$. The average front position and the standard deviation are plotted in figure 5 for 25×2^k, $k \in [\![0,8]\!]$ cells. For finer meshes, the computations require a lot of computational time, and the number of tries N_c becomes too small to obtain converged statistics (at least for the average front position). Convergence curves in figure 5 clearly show that the average and the standard deviation have an effective convergence rate of 1, which indicates that the probability function of the position of the front tends to a Dirac function centered on the exact front position. These results are also in agreement with the first result obtained in [8].

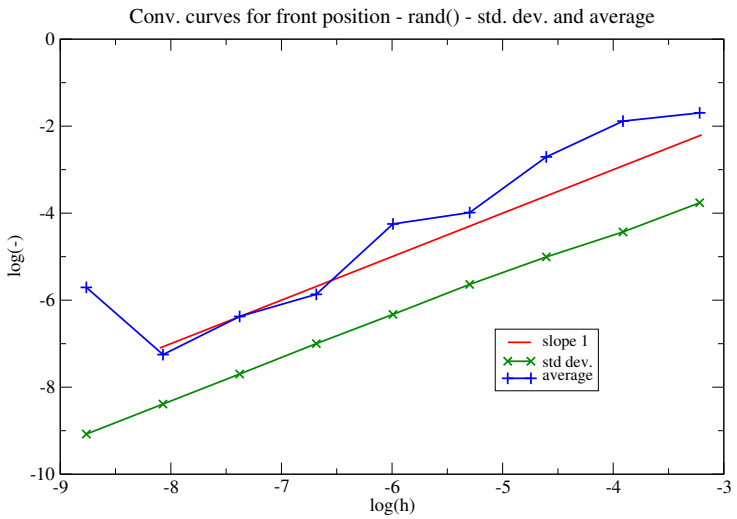

Figure 5: Convergence curves for the front position when using several rand() sequences. The logarithm of the distance between the exact front and the approximated average front is plotted in blue. The standard deviation of the position of the front is plotted in green.

4.3 Front propagation on non-uniform meshes

In this section, some theoretical results of section 3 are assessed for non-uniform meshes. The first test concerns the "odd-even" meshes. We choose here a ratio of two between two neighboring cells, i.e., $a = 2$ with the notation of section 3: $\Delta x_i = h$ for odd cells and $\Delta x_i = h/2$ for even cells. The convergence curves with respect to $h/2$ are plotted in figure 6a for the cases using 1 or 2 sequences, as described in section 3.3.1. These results highlight that the approximate solutions using a sole LCG sequence do not converge toward the correct solution. On the contrary, introducing a second sequence allows recovering the behavior observed on uniform meshes. For rand() sequences, no difference in terms of convergence is observed for 1 or 2 sequences, and order $1/2$ is recovered, as for the case of uniform meshes. The results obtained for the "odd-even" meshes are the same when cells are randomly mingled to create blocks of h-sized cells and blocks of $h/2$-sized cells. For such meshes, convergence curves are plotted in figure 6b. As with "odd-even" meshes, the use of two LCG sequences allows recovering convergence toward the correct solution. Moreover, the results computed for rand() sequences are not sensitive to the number of sequences.

Let us now turn to the case of block-shaped meshes. We consider here three values for γ: $1/3$, $1/2$, and $2/3$, and we set $\Delta x_i = h$ for odd blocks and $\Delta x_i = h/2$ for even blocks. This is a simpler setting than the one studied in section 3.3.1. The convergence curves are plotted in figure 7 for 1 sequence (on the left) and for 2 sequences (on the right). It can be observed that all the approximate solutions converge toward the exact one. When one sequence is used, the convergence rate clearly depends on the value of γ. We measured an effective convergence rate of: ~ 0.3 for $\gamma = 1/3$, ~ 0.62 for $\gamma = 1/2$, and ~ 0.9 for $\gamma = 2/3$. This is in rather good agreement with the bound found in section 3.3.1. With 2 sequences, the same type of results as those on uniform meshes are recovered, and the distance between the exact front and the approximated front is of order $h/2$. In fact, there are either 1 cell or 0 cells in terms of distance. Since the small cells have a size $h/2$ and the large cells have a size h, this explains the points that are above the line $err = h$ in figure 7 (on the right).

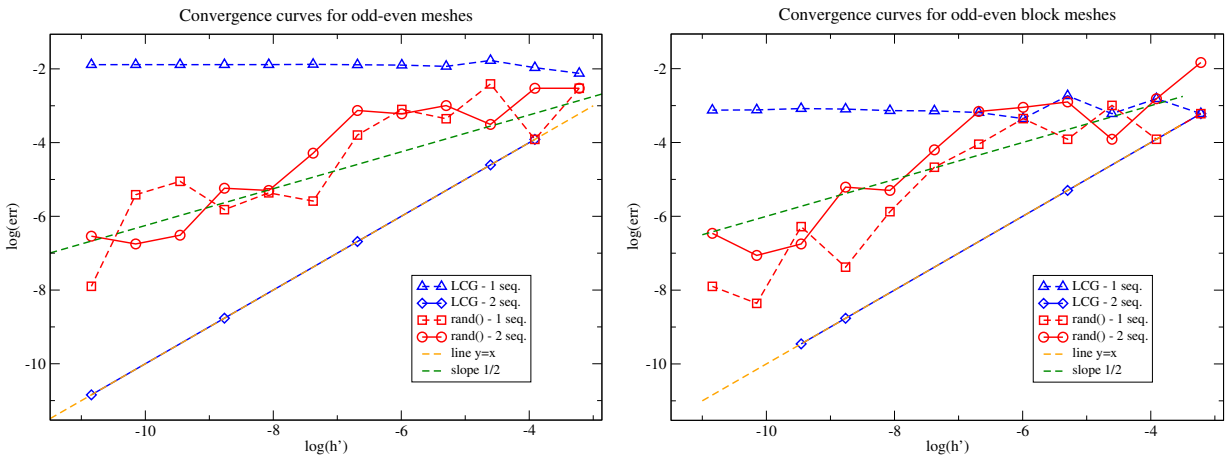

(a) Odd-even meshes with cells sizes $\Delta x_i = h/(1 - mod(i,2))$. (b) Meshes with randomly distributed cells with sizes h and $h/2$.

Figure 6: Convergence curves with respect to the small cell-size $h' = h/2$ for "odd-even" meshes for 1 sequence or 2 sequences. The red curves corresponds to the use of rand() sequences, while the blue ones corresponds to the LCG sequences.

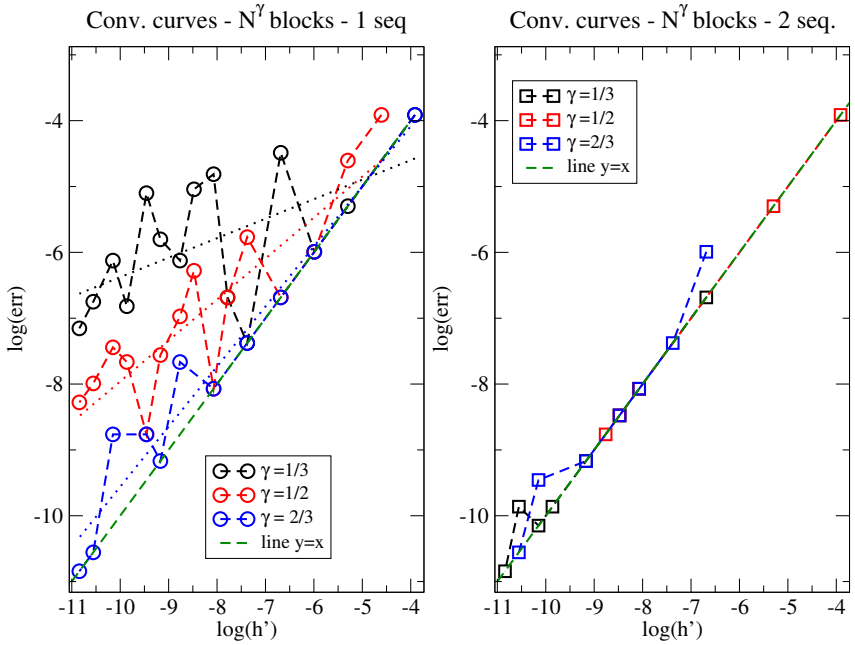

Figure 7: Convergence curves with respect to the small cell-size $h' = h/2$ for block-shaped meshes. On the right: approximate solution are obtained with 2 sequences; on the left: only one sequence is used.

5 Conclusion

In conclusion, the GRU scheme represents an interesting advancement in the numerical treatment of front propagation, particularly for complex geometrical settings. It offers substantial improvements over classical first-order schemes. The new theoretical results presented in this study further deepen the understanding of the behavior of the GRU scheme, in particular when using low-discrepancy sequences. Moreover, the numerical tests provide valuable insights for practical applications for which non-uniform/unstructured meshes are required. From a practical point of view, an important results is that convergence of the approximate solutions seems to be guaranteed provided that the number of mesh-size discontinuities increases slower that the number of cells.

6 Appendix

6.1 A technical lemma

Lemma. Let β be a real number in $[0,1]$. For all $s \geq 0$, we have: $e^{-\beta s}\left(1-\beta+\beta e^{s}\right) \leq e^{s^2/8}$.

Proof. The proof of the lemma is based on function $s \mapsto f(s) = s^2/8 - (-\beta s + \ln(1-\beta+\beta e^s))$. The first and second derivatives of $s \mapsto f(s)$ are respectively:

$$f'(s) = \frac{s}{4} - \left(-\beta + \frac{\beta e^s}{(1-\beta+\beta e^s)}\right) \quad \text{and} \quad f''(s) = \frac{1}{4} - \frac{(1-\beta)\beta e^s}{(1-\beta+\beta e^s)^2}.$$

Since $(1-\beta+\beta e^s)^2 = (1-\beta-\beta e^s)^2 + 4(1-\beta)\beta e^s$, we have the inequality $(1-\beta+\beta e^s)^2 \geq 4(1-\beta)\beta e^s$ and thus $f''(s) \geq 0$ for all $s \geq 0$. The derivative of f for $s = 0$ is $f'(0) = 0$, and then $f'(s) \geq 0$ for all $s \geq 0$. As $f(0) = 0$, we thus get that $f(s) \geq 0$ for all $s \geq 0$, which means that:

$$\forall s \geq 0, \quad s^2/8 \geq (-\beta s + \ln(1-\beta+\beta e^s)),$$

and thus that:

$$\forall s \geq 0, \quad e^{s^2/8} \geq e^{-\beta s}\left(1-\beta+\beta e^s\right).$$

This ends the proof of the lemma.□

References

[1] A. Bressan. Global solutions of systems of conservation laws by wave-front tracking. *Journal of mathematical analysis and applications*, 170(2):414–432, 1992.

[2] A. J. Chorin. Random choice solution of hyperbolic systems. *Journal of Computational Physics*, 22(4):517–533, 1976.

[3] P. Colella. Analysis of the effect of operator splitting and of the sampling procedure on the accuracy of glimm's method. *Report No. LBL-8774. California Univ., Berkeley (USA). Lawrence Berkeley Lab.*, 1978.

[4] P. Colella. Glimm's method for gas dynamics. *SIAM Journal on Scientific and Statistical Computing*, 3(1):76–110, 1982.

[5] B. Després, S. Kokh, and F. Lagoutière. Sharpening methods for finite volume schemes. *Handbook of Numerical Analysis*, 17:77–102, 2016.

[6] R. J. DiPerna. Global existence of solutions to nonlinear hyperbolic systems of conservation laws. 1976.

[7] T. Gallouët and R. Herbin. *Mesure, Intégration, Probabilités - 2nd Edition*. Ellipses, 2014.

[8] T. Gallouët and O. Hurisse. Convergence of a multidimensional Glimm-like scheme for the transport of fronts. *IMA Journal of Numerical Analysis*, 07 2021.

[9] T. Gallouët, O. Hurisse, and S. Kokh. A random choice scheme for scalar advection. *International Journal for Numerical Methods in Fluids*, 2023.

[10] J. Glimm. Solutions in the large for nonlinear hyperbolic systems of equations. *Communications on pure and applied mathematics*, 18(4):697–715, 1965.

[11] W. Hoeffding. Probability inequalities for sums of bounded random variables. *The collected works of Wassily Hoeffding*, pages 409–426, 1994.

[12] H. Holden, N. H. Risebro, and H. Sande. Front tracking for a model of immiscible gas flow with large data. *BIT Numerical Mathematics*, 50:331–376, 2010.

[13] O. Hurisse. On the use of Glimm-like schemes for transport equations on multidimensional domain. *International Journal for Numerical Methods in Fluids*, 93(4):1235–1268, 2021.

[14] T.-P. Liu. The deterministic version of the Glimm scheme. *Communications in Mathematical Physics*, 57(2):135–148, 1977.

[15] D. She, R. Kaufman, H. Lim, J. Melvin, A. Hsu, and J. Glimm. Front-tracking methods. *Handbook of Numerical Analysis*, 17:383–402, 2016.